

Effect of substrate temperature on structural and optical properties of nickel tungsten oxide thin films

K. S. Usha · R. Sivakumar · C. Sanjeeviraja

Received: 17 October 2014 / Accepted: 10 November 2014 / Published online: 14 November 2014
© Springer Science+Business Media New York 2014

Abstract In this work, we present the substrate temperature induced change in the structural, optical, vibrational and luminescence properties of mixed NiO:WO₃ (95:5) thin films deposited on glass substrates by rf magnetron sputtering technique. X-ray diffraction analysis revealed the onset of crystallization of the films occurred at 300 °C. The average optical transmittance of the films varied between 91 and 97 % in the visible region. The refractive index and extinction coefficient of films are found to decrease with increasing substrate temperature. It was observed that the dispersion data obeyed the single oscillator of the Wemple-DiDomenico model, from which the dielectric constants, ratio between free carrier density and free carrier effective mass, plasma frequency, oscillator energy, oscillator strength, and dispersion energy parameters of NiO:WO₃ films were calculated and reported for the first time due to variation in substrate temperature during deposition by rf magnetron sputtering. The micro-Raman result shows two broad peaks corresponding to one-phonon LO mode at 570 cm⁻¹ and two-phonon LO mode at 1,100 cm⁻¹ due to the vibrations of Ni–O bonds and the peak found at 870 cm⁻¹ belongs to the W–O mode. Room

temperature photoluminescence (RTPL) study exhibits two characteristic emission peaks at 3.32 eV (374 nm) and 2.93 eV (423 nm), which corresponding to the transition of 3d⁸ Ni²⁺ ions. We have made an attempt to discuss and correlate these results with the light of possible mechanisms underlying the phenomena.

1 Introduction

Many of transition metal oxide thin films exhibit an electrochromic (EC) effect as they change their optical transmittance upon charge insertion or extraction. Among the transition metal oxides, nickel oxide (NiO) and tungsten oxide (WO₃) are extensively studied electrochromic materials. Nickel oxide thin films are considered as an important candidate due to their technological applications as an antiferromagnetic layer, p-type transparent conducting film, as an active electrode in electrochromic devices, functional sensing layer for developing chemical sensors, etc. [1]. On the other hand, tungsten oxide has been used as an outstanding electrochromic material for smart-window applications, anti-glare rear view mirrors for automobiles and gas sensors owing to its excellent optical and electrochromic properties [2].

Now-a-days, research efforts have been focused to find a new optical and EC material with improved optical and electro-optical characteristics, which find applications in integrated optics such as optical modulation, optical information display, and optical data storage [3]. It may be mentioned that the mixed oxide thin films possess better electrochromic properties than pure oxides because of greater optical response. Binary nickel-tungsten oxides, either made of tungsten mixed nickel oxide [4, 5] or nickel mixed tungsten oxide [6] thin films have been found to

K. S. Usha
Department of Physics, Alagappa University, Karaikudi 630 004,
India

R. Sivakumar (✉)
Directorate of Distance Education, Alagappa University,
Karaikudi 630 004, India
e-mail: krsivakumar1979@yahoo.com

C. Sanjeeviraja
Department of Physics, Alagappa Chettiar College
of Engineering and Technology, Karaikudi 630 004, India

yield better electrochromic properties than those of the pure oxides. Lee et al. [7] reported that the lithium ion insertion and the current density of NiO:WO₃ films are greater than NiO.

Different techniques are employed to grow metal oxide thin films, viz. thermal evaporation, [8] electron beam evaporation, [9] spray pyrolysis, [10] reactive pulsed laser ablation technique, [11] and sputtering [12]. Among these techniques, radio frequency (rf) sputtering is the major industrial process due to its high deposition rate, high volume, and large area uniformity. In the present work, we have prepared NiO:WO₃ (95:5) films by rf magnetron sputtering technique. To the best of our knowledge, no detailed report has been devised on the optical parameters of NiO:WO₃ thin films due to the variation of substrate temperatures while film preparation. Therefore, such a study would be important to develop interesting technological optical devices such as special optical communication and spectral dispersion devices. Hence, our present work provides detailed information about various optical parameters such as absorption coefficient, optical band gap, optical dispersion energies, high frequency dielectric constant, average values of oscillator strength, plasma frequency, non-linear optical susceptibility, etc. of NiO:WO₃ thin film. In addition, the results of room temperature photoluminescence (RTPL), micro-Raman and X-ray diffraction studies are discussed in detail.

2 Experimental details

Mixed NiO:WO₃ (95:5) thin films were prepared on pre-cleaned glass substrate by rf magnetron sputtering (HINDHIVAC; Planar Magnetron RF/DC Sputtering Unit Model-12" MSPT) using NiO:WO₃ (95:5) target (99.99 % purity) of 5 cm diameter. Depositions were carried out under the chamber pressure of 5×10^{-3} mbar. The distance between target and substrate was ~ 6 cm. The films were deposited at constant (100 W) rf power with various substrate temperatures ($T_{\text{sub}} = 100, 200$ and 300 °C) for about 30 min duration. The thickness of the film was measured by Stylus profilometer (Mitutoyo, SJ-301). The structural property of NiO:WO₃ thin film was studied by X-ray diffraction (XRD) using Cu-K_α ($\lambda = 0.154$ nm) radiation source (X' pert Pro PANalytical) over a 2θ scan range of 10–80°. The effect of substrate temperature on the optical properties of NiO:WO₃ films were studied using UV–Vis–NIR spectrophotometer (JASCO; V-670) in the wavelength range of 300–2,500 nm. Micro-Raman studies were done using STR Raman spectroscopy. Room temperature photoluminescence (RTPL) study was performed using Varian Cary Eclipse fluorescence spectrophotometer.

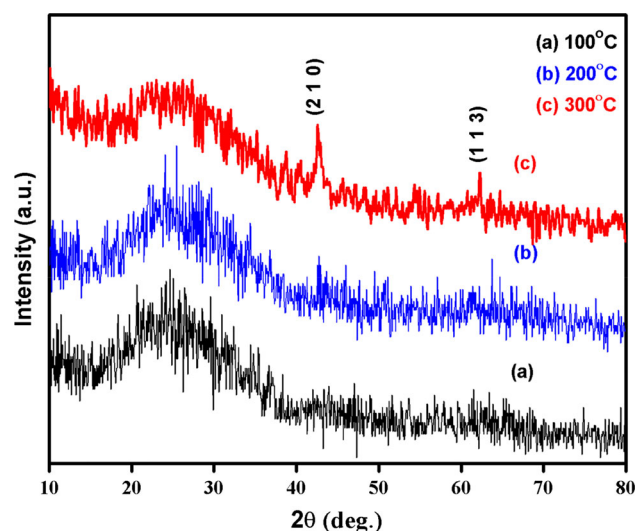


Fig. 1 XRD patterns of NiO:WO₃ thin films deposited at various substrate temperatures

3 Results and discussion

3.1 Structural studies

Thickness of NiO:WO₃ thin films coated at 100, 200 and 300 °C are found to be 0.85, 0.80, 0.75 μm. The rf sputter deposited NiO:WO₃ thin films (on glass substrates) have been subjected to X-ray diffraction to analyze their structural behavior. Figure 1 shows the X-ray diffraction patterns of NiO:WO₃ thin films deposited on microscopic glass substrates at different substrate temperatures. It is observed that the films deposited up to the substrate temperature of 200 °C are amorphous in nature (Fig. 1a, b), this is because of incomplete formation of ordered NiO:WO₃ species on the substrate surface due to the low thermal energy at lower substrate temperature (T_{sub}). When the film is deposited at higher substrate temperature ($T_{\text{sub}} = 300$ c), the onset of crystallization occurred in the film and it is evident from the diffraction peaks observed at 42.5° and 62.2° (Fig. 1c). The observed d spacings are matched well with monoclinic NiO:WO₃ (JCPDS Card No. 72-0480).

3.2 Optical studies

The substrate temperature induced change in optical absorption and transmission spectra of NiO:WO₃ films recorded in the wavelength range of 300–2,500 nm are shown in Figs. 2 and 3, respectively. From the absorption spectra (Fig. 2), it can be seen that the sharp absorption edge in the ultraviolet (UV) region. This absorption edge in the UV region is due to band-to-band absorption, which

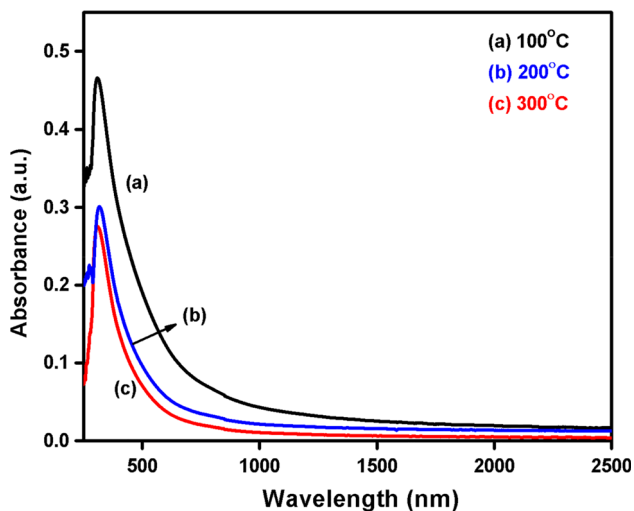


Fig. 2 Absorbance spectra of NiO:WO₃ thin films

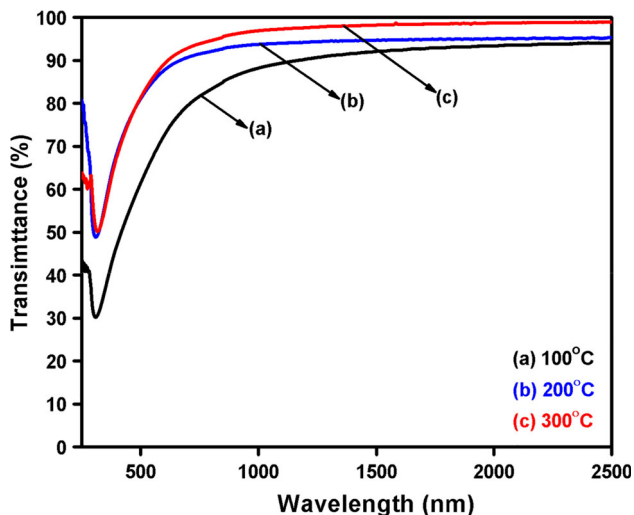


Fig. 3 Transmittance spectra of NiO:WO₃ thin films

involves transition of an electron from the valence band to the conduction band. In addition, decrease in absorption with increasing T_{sub} may be attributed to the decrease in the electronic transitions. Also, the absorption edge becomes sharper with increasing T_{sub} which may be due to the decrease in scattering loss for thinner film [13]. Further, the slight shift in absorption edge towards lower wavelength (blue shift) region revealed the systematic increase in barrier width. It was reported that the absorption of NiO and/or WO₃ in the wavelength longer than 400 nm is associated with an excess of oxygen (defects) in the lattice [14, 15]. In the present work, the steeper increase in optical transmission at UV region may be due to the reduction in defect density [16]. It is observed from Fig. 3 that the

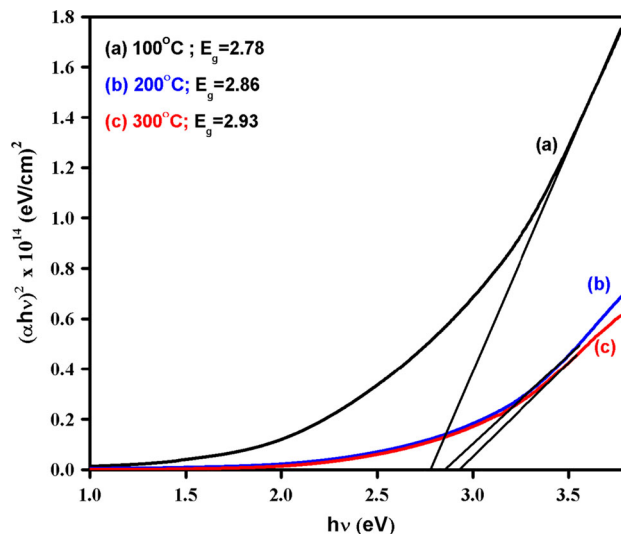


Fig. 4 Tauc plot of NiO:WO₃ thin films

increase in transmittance with increasing substrate temperature may be due to the decreased defect density and the decrease in optical scattering of the film. The average transmittance of the film varies between 91 and 97 %.

The optical band gap of the films is determined by applying the Tauc model [17],

$$\alpha h\nu = A(h\nu - E_g)^n \tag{1}$$

where A is energy independent constant, E_g is the band gap corresponding to a particular transition occurring in the film, ν is transition frequency and the exponent n characterizes the nature of the band transition. For crystalline semiconductors, $n = 1/2, 2, 3/2, 3$ values corresponding to the allowed direct, allowed indirect, forbidden direct, and forbidden indirect transitions, respectively. Since NiO is a direct band gap system, the relationship between $(\alpha h\nu)^2$ and $h\nu$ is expected to show the linear behavior as shown in Fig. 4. The E_g value was obtained by extrapolating the linear portion to the photon energy axis. It is found that the optical energy band gap increases with substrate temperature (2.78–2.93 eV). Generally, in doped semiconductors, the Fermi level lies between the conduction and valence bands. According to the Moss-Burstein shift in semiconductor [18, 19], the electrons in the conduction band gets more populated which pushes the Fermi level to higher in energy. For a degenerate semiconducting material, electronic transition is possible only above the Fermi level. Since all the states below the Fermi level are occupied states, it needs higher energy for electronic transition. Hence, we observe an increase in the apparent band gap with the addition of WO₃ into the NiO matrix. The increase in E_g values with T_{sub} may also be due to removal of excess oxygen in the prepared film [15].

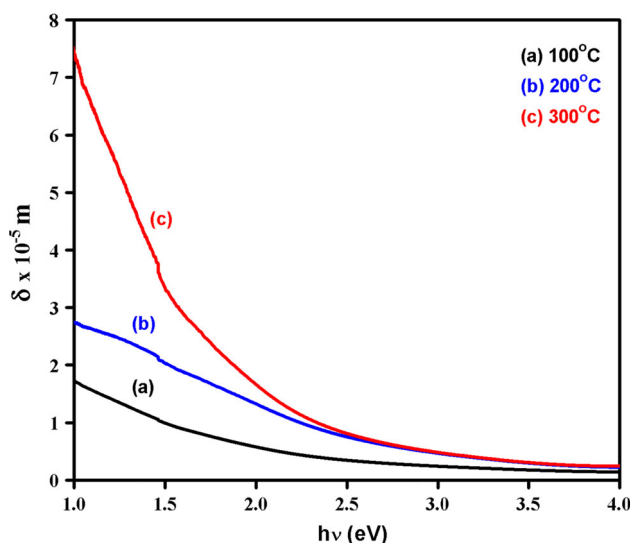


Fig. 5 Variation of skin depth with photonic energy of NiO:WO₃ thin films at different substrate temperatures

The inverse of the absorption coefficient $\delta = 2/\alpha = c/\omega k$ is known as the skin depth (δ). The intensity $I = I_0/e^{-x/\delta}$, and hence δ , is a measure of the distance of penetration of the optical beam into the medium before the beam is dissipated. In practice, δ has a very small value (in the order of μm), indicating that an optical beam incident on material penetrates only a short distance into the surface. It is seen from Fig. 5 that the skin depth increases with increasing T_{sub} . The absorption coefficient near the band edge shows an exponential dependence on photon energy and this dependence is given as follows [20],

$$\alpha = \alpha_o \exp\left(\frac{h\nu}{E_u}\right) \quad (2)$$

where α_o is a constant and E_u is the width of the band tail of the localized states at the optical band gap. The Urbach energy, E_u , can be determined from the plot of $\ln(\alpha)$ versus $h\nu$ (graph not shown here) and the values are listed in Table 2. In general, the Urbach edge is determined by the degree of disorder (e.g. charged impurities) and/or structural defects (e.g. broken or dangling bonds, vacancies, non-bridging atoms, or chain ends) in the semiconductor material [21]. Hence, decrease in E_u values with increasing substrate temperature (Table 2) revealed the reduced defects in coated film. Also, it is known that the optical band gap is reversely related to the disorder in the film. Thus, decrease in E_u values can be correlated with increase in E_g values.

Refractive index (n) is an important factor in optical communication and in designing spectral dispersion, optical and optoelectronic devices. The refractive index dispersion data below the interband absorption edge are

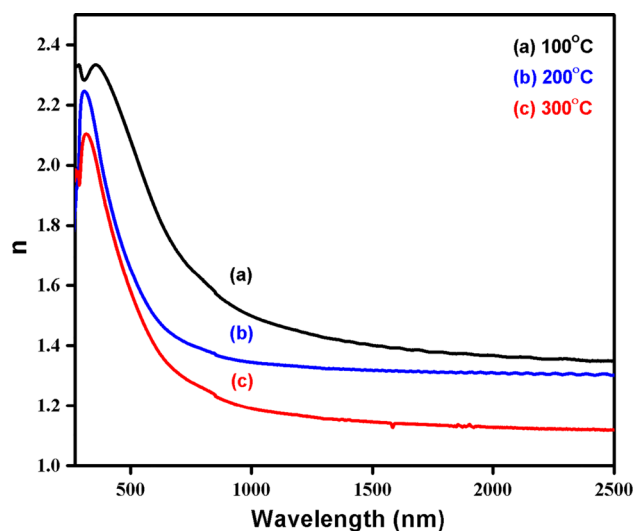


Fig. 6 Variation of refractive index with wavelength of NiO:WO₃ thin films at different substrate temperatures

much important for technological applications of the optical materials, since, the dispersion energy is related to the optical conductivity and optical transition strengths. Generally, various approaches (like Cauchy, Sellmeier, Lorentz, Swanapoel, etc.) have been used to calculate the refractive index of thin films employing the transmittance data [22]. In addition, Al-Ghamdi et al. [23, 24] have reported a simple method to evaluate the n and k of NiO thin films using the optical data. The refractive index, n and the extinction coefficient, k of NiO:WO₃ films were calculated using the following relations [23, 24]

$$n = \left(\frac{1+R}{1-R}\right) - \sqrt{\frac{4R}{(1-R)^2} - k^2} \quad (3)$$

$$k = \frac{\alpha\lambda}{4\pi} \quad (4)$$

where R is the reflectance of the film and λ is the wavelength of the incident beam. Figure 6 shows the substrate temperature induced change in refractive index, n of NiO:WO₃ thin film as a function of wavelength. The refractive index of NiO:WO₃ thin film decreases with increasing substrate temperature indicating the decrease in densification (or packing density) of the film. Whereas, Fig. 7 shows the variation in extinction coefficient, k as a function of wavelength and substrate temperature. The decrease in k value with increasing substrate temperature may be due to the decrease in surface roughness of the film, which decreases the scattering losses thereby increasing the transmitting ability. This inference is in agreement with the transmittance data.

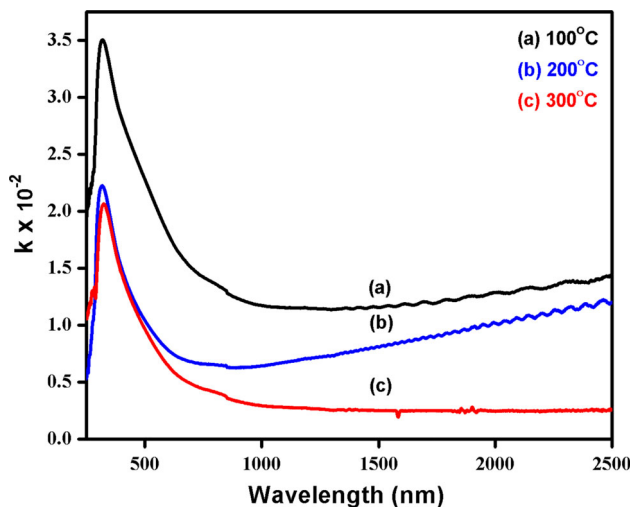


Fig. 7 Variation of extinction coefficient with wavelength of NiO:WO₃ thin films at different substrate temperatures

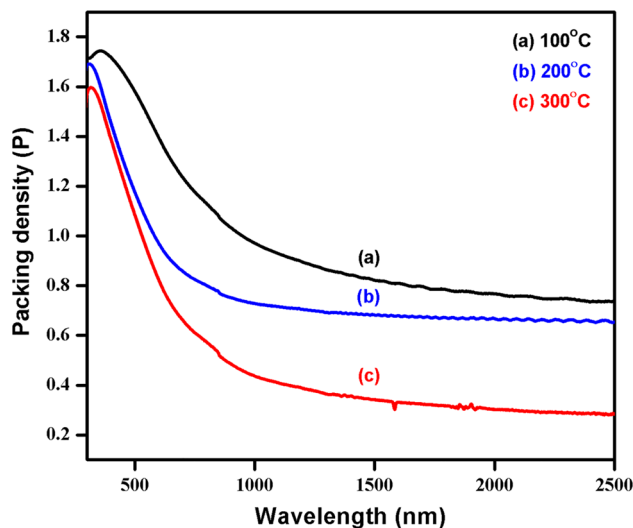


Fig. 8 Plot of packing density versus wavelength of NiO:WO₃ thin films

Generally, for a semiconducting material the refractive index (typically for $\hbar\omega < E_g$) decreases with increasing energy band gap or vice versa. Several expressions have been devised to relate n and E_g . Based on Moss [25] atomic model, n and E_g can be related by the expression $n^4 E_g \approx K$, where K is a constant ($K \approx 100$ eV). According to Hervé-Vandamme relationship [26], the n and E_g can be expressed as

$$n^2 = 1 + \left(\frac{A}{E_g + B} \right)^2 \tag{5}$$

where A and B are constants ($A = 3.6$ eV and $B = 3.4$ eV). Our result agrees well with the above said expressions (i.e. the refractive index values decreased with increasing band gap). This is evident from the increase in E_g (Fig. 4) and decrease in refractive index (Fig. 6) as a function of increasing substrate temperature.

The refractive index plays an important role in determining packing density of the film. The packing density can be detected from the Bragg and Pippard model [27], which was later modified by Macleod [28] as given below:

$$n^2 = \frac{[(1-p)n_v^4 + (1+p)n_v n_s^2]}{(1+p)n_v^2 + (1-p)n_s^2} \tag{6}$$

where n is the refractive index of the prepared film, n_s is the substrate refractive index and n_v is the void refractive index (equal to the one for air) and p is packing density. Figure 8 represents the plot of packing density as a function of wavelength and substrate temperature. From the figure it can be seen that the packing density of the film decreases with increasing substrate temperature which may be due to decrease in refractive index value.

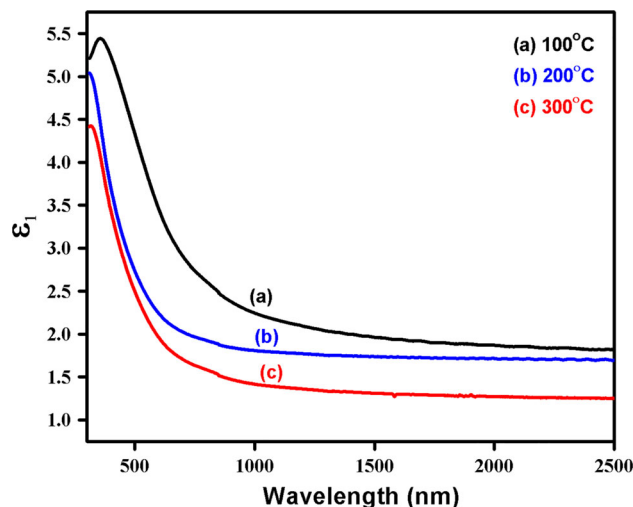


Fig. 9 Plot of real part of dielectric constant versus wavelength of NiO:WO₃ thin films

We have also evaluated the real and imaginary parts of the complex dielectric constant, ϵ_1 and ϵ_2 of NiO:WO₃ thin films using the following equations [29],

$$\epsilon_1 = n^2 - k^2 \tag{7}$$

$$\epsilon_2 = 2nk \tag{8}$$

The respective changes in ϵ_1 and ϵ_2 values as a function of wavelength are shown in Figs. 9 and 10. It is noticed that the real and imaginary parts of dielectric constants increase with decreasing substrate temperature indicating the

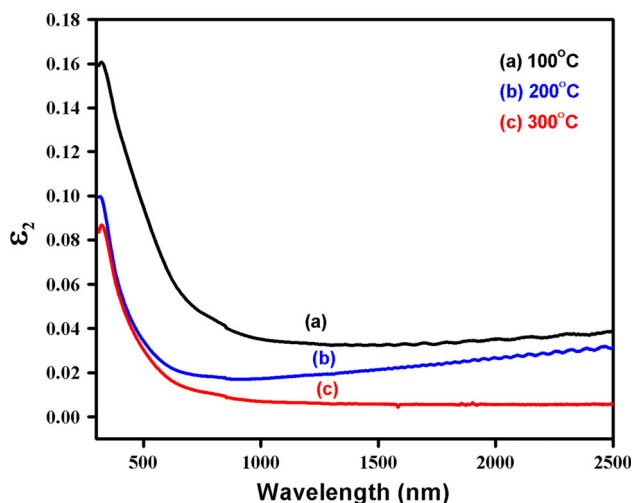


Fig. 10 Plot of imaginary part of dielectric constant versus wavelength of NiO:WO₃ thin films

enhancement in optical response (i.e. decrement in the dissipative rate of the wave).

When photons falls on a semiconducting material it excites electron from the valence band to conduction band, these electrons take part in conductivity process (optical conductivity), called photonic effect. The variation in optical conductivity (σ_{op}) as a function of photon energy ($h\nu$) is shown in Fig. 11 and it can be determined using the following relation: [30]

$$\sigma_{op} = \frac{\alpha n c}{4\pi} \quad (9)$$

where c is the velocity of light. It is clear from Fig. 11 that the optical conductivity decreases with increasing substrate temperature, which may be due to the nickel vacancies in the films. The real part of dielectric constant in higher wavelength region can be written as follows [31]

$$\varepsilon_1 = \varepsilon_L - \left(\frac{e^2 N}{4\pi c^2 \varepsilon_0 m^*} \right) \lambda^2 \quad (10)$$

and

$$\frac{N}{m^*} = \left(\frac{\varepsilon_\infty \varepsilon_0}{e^2} \right) \omega_p^2 \quad (11)$$

where, ε_L is the lattice dielectric constant, e is the electronic charge, c is the velocity of light, ε_0 is free space dielectric constant (8.854×10^{-12} F/m), N/m^* is the ratio between free carrier density and free carrier effective mass and ω_p is the plasma resonance frequency of all valence electrons involved in the optical transitions. The nature of the dispersion of n^2 as a function of wavelength λ^2 for different substrate temperatures is shown in Fig. 12. The respective intercept and slope values evaluated from Fig. 12 gives ε_L and N/m^* and they are presented in Table 1. It is observed

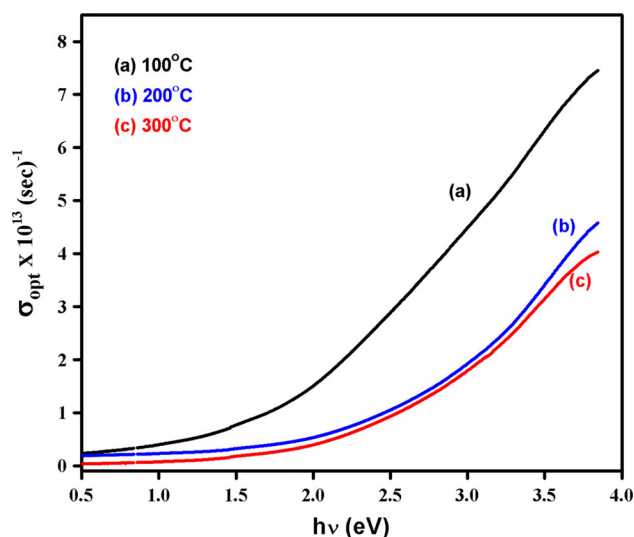


Fig. 11 Variation of optical conductivity with photon energy of NiO:WO₃ thin films at different substrate temperatures

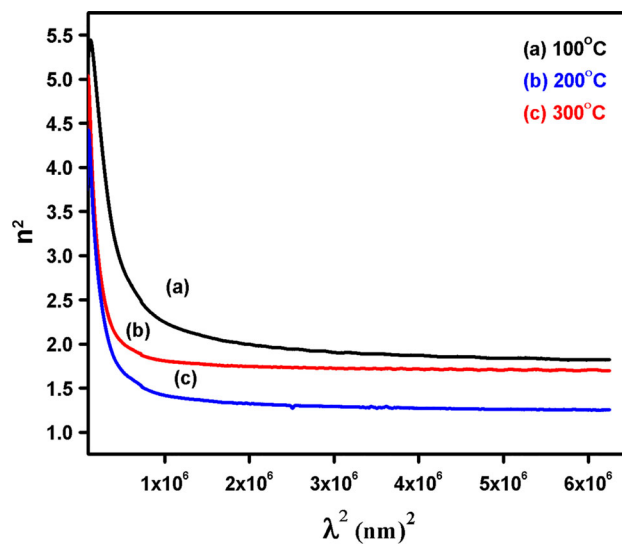


Fig. 12 Plot of n^2 versus λ^2 of NiO:WO₃ thin films

that both ε_L and N/m^* values decreased with increasing substrate temperature due to the reduction in free carrier density. The plasma resonance frequency (ω_p) evaluated using Eq. (11), decreases with increasing substrate temperature (Table 1). This may be due to the decrease in free carrier concentration, which agrees well with optical and N/m^* results.

The refractive index n can also be analyzed to determine the oscillator strength S_o for NiO:WO₃ thin films. The refractive index is represented by a single Sellmeier oscillator at low energies [32]:

Table 1 Optical dielectric parameters of NiO:WO₃ films

Substrate temperature (°C)	ϵ_L	ϵ_∞	n_0	λ_o	$S_o \times 10^{12}$	$N/m^* \times 10^{40}$ ($cm^{-3}g^{-1}$)	ω_p (s ⁻¹) $\times 10^6$
100	2.15	2.14	1.46	473	5.14	1.34	6.23
200	1.78	1.76	1.32	392	5.07	1.32	6.20
300	1.48	1.61	1.26	378	3.35	1.20	5.80

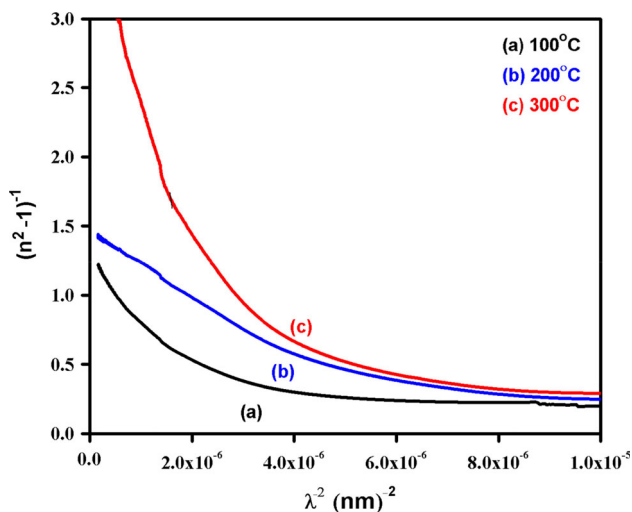


Fig. 13 Plot of $(n^2 - 1)^{-1}$ versus λ^{-2} of NiO:WO₃ thin films

$$\frac{(n_0^2 - 1)}{(n^2 - 1)} = 1 - \left(\frac{\lambda_o}{\lambda}\right)^2 \tag{12}$$

Equation (12) can also takes the form:

$$(n^2 - 1) = \frac{S_o \lambda_o^2}{\left(1 - \frac{\lambda_o^2}{\lambda^2}\right)} \tag{13}$$

Furthermore, the average oscillator strength S_o can be deduced from the following equation:

$$S_o = \frac{(n_o^2 - 1)}{\lambda_o^2} \tag{14}$$

Here n_o is the static refractive index; λ_o is the average interband oscillator wavelength which provides information about the structure and density of the material. High frequency dielectric constant (ϵ_∞) can be evaluated by plotting $(n^2 - 1)^{-1}$ versus λ^{-2} as shown in Fig. 13 with respect to substrate temperature. The intersection with $(n^2 - 1)^{-1}$ axis gives high frequency dielectric constant (ϵ_∞) and it is presented in Table 1. The value of n_0 was also evaluated from this graph (Fig. 13) which varies from 1.46 to 1.26 (Table 1), indicating the reduction in density of the film with raise in substrate temperature, which is in

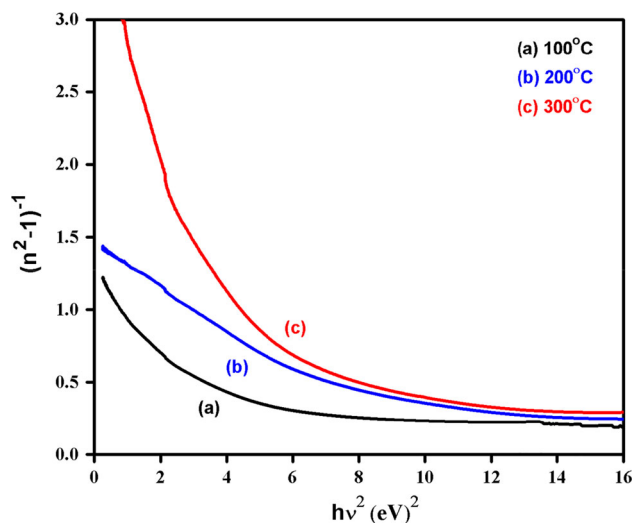


Fig. 14 Plot of $(n^2 - 1)^{-1}$ versus $(hv)^2$ of NiO:WO₃ thin films

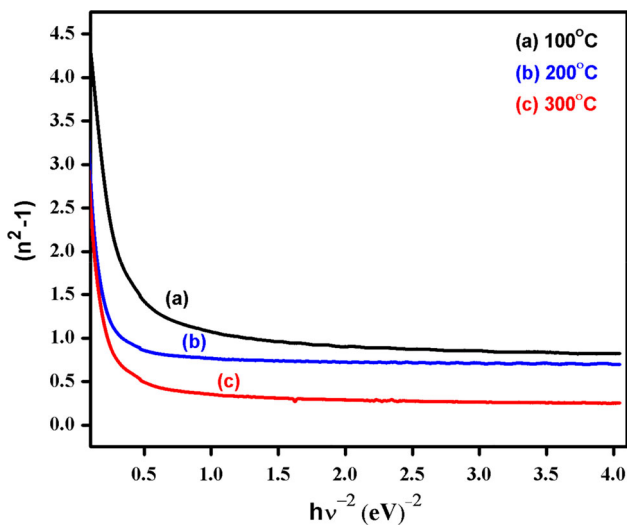
agreement with the decrease in refractive index. The calculated values of, n_0 , ϵ_∞ , λ_o and S_o are shown in Table 1. It is found that the ϵ_∞ decreases with increasing substrate temperature as in the case of ϵ_L . The values of ϵ_∞ and ϵ_L are matched with each other and the very small difference between them may be due to the lattice vibrations and bounded carriers in an empty lattice which are in the transparent region [33, 34].

The dispersion energy is important for communication and spectral analysis device design. Wemple and DiDomenico (WD) [34] have developed a refractive index dispersion model below the optical band gap using the single oscillator approximation. This model plays an important role in analyzing the behavior of refractive index of the film. Two important parameters, the oscillator energy E_o denoting the average excitation energy for electronic transitions and the dispersion energy E_d which represents the strength of interband optical transitions, can be evaluated from the following relation

$$n^2 - 1 = \frac{E_o E_d}{E_o^2 - (hv)^2} \tag{15}$$

Table 2 Dispersion energy parameters of NiO:WO₃ films

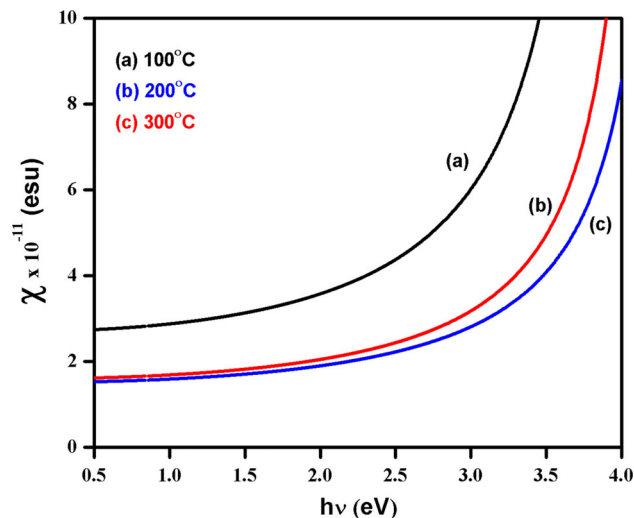
Substrate temperature (°C)	E_o (eV)	E_d (eV)	E_l (eV)	E_g (eV)	E_u (eV)	E_o/E_g	M_{-1}	M_{-3} (eV) ⁻²
100	4.042	8.07	0.344	2.78	1.09	1.45	1.99	0.122
200	4.252	5.01	0.214	2.86	0.90	1.48	1.17	0.065
300	4.410	4.92	0.170	2.93	0.67	1.50	1.11	0.057

**Fig. 15** Plot of $(n^2 - 1)$ versus $(hv)^{-2}$ of NiO:WO₃ thin films

The parameter E_d is related to the nearest neighbor cation co-ordination, anion valence, ionicity, and the effective number of dispersion electrons. A plot of $(n^2 - 1)^{-1}$ versus $(hv)^2$ is shown in Fig. 14. The values of E_d and E_o are obtained from the intercepts, and slopes of the curves, respectively and the values are presented in Table 2. The values of E_o was found to increase with increasing T_{sub} which could be attributed to the decrease in number of scattering center and also due to the increase in band gap energy. Whereas, the E_d values decrease with increasing T_{sub} which could be attributed to the decrease in co-ordination number of the atoms due to the addition of tungsten oxide and also due to decrease in average transition strength [35]. As mentioned above, the oscillator energy, E_o , is related to the optical band gap (E_g) by $E_o \approx 1.5E_g$, as suggested by WD model [34]. It is evident from Table 2 that the average ratio of $E_o/E_g \approx 1.5$, which shows an agreement with this relation.

Another interesting optical parameter known as the lattice energy (E_l), which gives information about the strength of the bonds, can be evaluated using the following relation [36]

$$n^2 - 1 = \left(\frac{E_o E_d}{E_o^2 - E^2} \right) - \frac{E_l^2}{E^2} \quad (16)$$

**Fig. 16** Variation of nonlinear optical susceptibility with photonic energy of NiO:WO₃ thin films as a function of substrate temperature

where E_l is the lattice energy. At longer wavelength, where $E_o^2 \gg E^2$, Eq. (16) takes the form as

$$n^2 - 1 = \left(\frac{E_d}{E_o} \right) - \frac{E_l^2}{E^2} \quad (17)$$

Slope of the graph between $(n^2 - 1)$ and $(hv)^{-2}$ (Fig. 15) gives $-E_l^2$. The calculated E_l values are summarized in Table 2, and are found to decrease with increasing substrate temperature indicating the decrement in strength of the bonds. The moments M_{-1} and M_{-3} of the optical transitions were evaluated using the following relations [33]

$$E_o^2 = \frac{M_{-1}}{M_{-3}} \quad (18)$$

$$E_d^2 = \frac{M_{-1}^3}{M_{-3}} \quad (19)$$

The evaluated values of M_{-1} vary from 1.99 to 1.11 (dimensionless) and M_{-3} lies between 0.122 and 0.057(eV)⁻² (Table 2).

The third order optical nonlinear susceptibility $\chi^{(3)}$ gives the information about the strength of the chemical bonds between the molecules and was calculated using the following relation [23, 24, 37]:

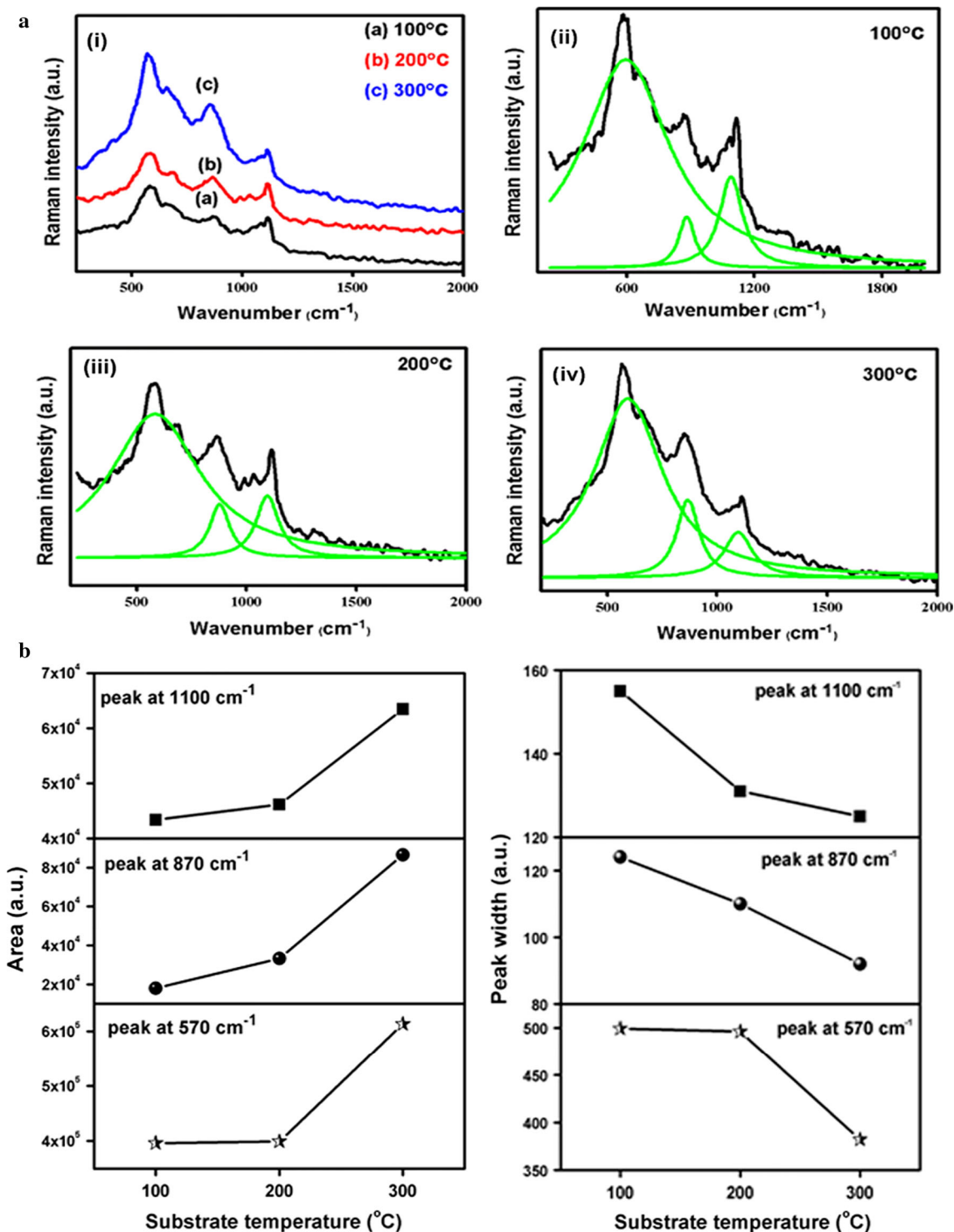


Fig. 17 a (i) Micro-Raman spectra of NiO:WO₃ thin films deposited at various substrate temperatures (ii) Gaussian fit for 100 °C (iii) Gaussian fit for 200 °C (iv) Gaussian fit for 300 °C and **b** Variation of area and peak width of different Raman peaks with substrate temperature

$$\chi^{(3)} = A(\chi^{(1)})^4 = A \left(\frac{E_o E_d}{4\pi [E_o^2 - (hv)^2]} \right) \quad (20)$$

where A is a constant, $A = 1.7 \times 10^{-10}$ esu and $\chi^{(1)}$ is the linear optical susceptibility. From Fig. 16 it can be seen that $\chi^{(3)}$ decreases with increasing T_{sub} which revealed the decreased strength of the chemical bonds between the

molecules of NiO:WO₃ thin films. This hypothesis is consistent with the result of lattice energy (E_l).

3.3 Vibrational studies

Figure 17 a(i) shows the room temperature Raman spectra of mixed NiO:WO₃ films deposited at different substrate temperatures. In order to have better insight on the quantitative information of Raman lines with substrate temperature, we have fitted the Raman data of individual sample using Gaussian fit, as shown in Fig. 17a(ii–iv), along with the measured data. The Raman spectra show two broad peaks corresponding to one-phonon longitudinal optic (LO) mode at 570 cm⁻¹ and two-phonon LO mode at 1,100 cm⁻¹ due to the vibrations of Ni–O bonds. In general, NiO:WO₃ or NiWO₄ has a Raman signal around 850–950 cm⁻¹ and this peak can easily be detected in thin films [38]. Hence, the observed Raman band found at 870 cm⁻¹ belongs to W–O vibrational mode. However, the relative intensity (peak height) of the Raman lines increases with increasing substrate temperature. This may be due to decreased lattice disorder in the film. In addition, the Raman peak widths are found to decrease (Fig. 17b) with increasing substrate temperature, since the phonon lifetime increases whenever there is a decrease in the defect density in the lattice [39]. Besides, increase in the peak area (Fig. 17b) of different Raman lines can be correlated with an increase in the optical band gap [39]. Further, the broad Raman peaks indicate the amorphous nature of NiO:WO₃ films, which is in line with X-ray diffraction result.

3.4 Photoluminescence studies

Photoluminescence (PL) is an effective non-destructive technique, which can be used to study the optical, electronic structure, and photochemical properties of a semiconductor. Literature survey shows that very sparse reports are existing on the PL study of mixed NiO:WO₃ thin films. Figure 18 shows the room temperature photoluminescence (RTPL) spectra of NiO:WO₃ thin films deposited at different substrate temperatures. The two characteristic RTPL emission peaks (for $T_{\text{sub}} = 100$ °C) appear at 3.32 eV (374 nm) and 2.93 eV (423 nm) when excited at a wavelength of 270 nm. It was reported that the radiative recombination of carriers in NiO bulk consists of two photoemission maxima, one at 3.2 eV and a larger one at 2.8 eV [40]. The origin of the main UV emission peak at 374 nm may be attributed to the electronic transition of 3d⁸ Ni²⁺ ions [41]. Adler and Feinleib reported that the series of peaks below 4 eV corresponding to the intraionic 3d⁸–3d⁸ transitions of Ni²⁺ [42]. Hence, the visible emission peak at 423 nm also belongs to the transition of 3d⁸ Ni²⁺ ions. The RTPL intensity, provides information about the

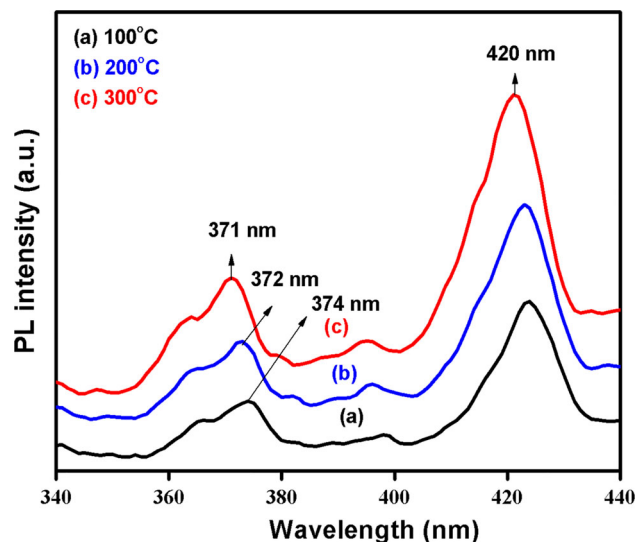


Fig. 18 Room temperature photoluminescence spectra of NiO:WO₃ thin films

quality of surfaces and interfaces, is found to increase with substrate temperature which may be due to the following reasons. The raise in intensity may be due to the increase in Ni²⁺ ions. It may be mentioned that the oxygen vacancies act as an electron capturer, causes decrement in the recombination process by which the PL intensity decreases [43, 44]. Hence, the raise in PL intensity may also be due to decreased oxygen vacancies (defects) which agree well with optical absorption, Urbach energy and Raman results. In addition, the added tungsten metal acts as an electron capturer and the film reaches to near stoichiometric ratio (by which enhances recombination process) with increasing T_{sub} , therefore it takes part in enhancing the PL intensity [43]. The blue shift in PL peaks with increasing T_{sub} may be due to the change in energy band gap values. Moreover, this blue shift in PL peaks reveals the possibility of using NiO:WO₃ films for tunable infra-red detectors [45].

4 Conclusion

The effect of substrate temperature on various properties of rf magnetron sputtered NiO:WO₃ thin films were studied in detail. X-ray diffraction study reveals the amorphous nature of film at low temperature and the onset of crystallization at 300 °C. Transmittance of the films is found to increase with increasing T_{sub} owing to the decreased oxygen vacancies. The energy band gap values are found to increase with substrate temperature. We have also discussed in detail about the various optical parameters such as n , k , ϵ_1 and ϵ_2 , E_o , E_d , E_l , lattice dielectric constant ϵ_L ,

high frequency dielectric constant ϵ_∞ , the average values of oscillator strength S_o , wavelength of single oscillator λ_o , plasma frequency ω_p and non-linear optical susceptibility $\chi^{(3)}$. Raman study shows two broad peaks corresponding to one-phonon LO mode at 570 cm^{-1} and two-phonon LO mode at $1,100\text{ cm}^{-1}$ due to the vibrations of Ni–O bonds and the peak found at 870 cm^{-1} belongs to the W–O mode. The photoluminescence study shows two characteristic emission peaks at 3.32 eV (374 nm) and 2.93 eV (423 nm) due to the transition of $3d^8\text{ Ni}^{2+}$ ions.

Acknowledgments One of the authors (K. S. Usha) gratefully acknowledges the Department of Science and Technology, New Delhi, India for the financial assistance rendered through Innovation in Science Pursuit for Inspired Research (INSPIRE).

References

1. B. Subramanian, M. Mohamed Ibrahim, V. Senthilkumar, K.R. Murali, V.S. Vidhya, C. Sanjeeviraja, M. Jayachandran, Optoelectronic and electrochemical properties of nickel oxide (NiO) films deposited by DC reactive magnetron sputtering. *Phys. B* **403**, 4104–4110 (2008)
2. M.M. Hasan, A.S.M.A. Haseeb, H.H. Masjuki, Structural and mechanical properties of nano structured tungsten oxide thin films. *Sur. Eng.* **28**, 778–785 (2012)
3. M. Yin, H.P. Li, S.H. Tang, W. Ji, Determination of nonlinear absorption and refraction by single Z-scan method. *Appl. Phys. B: Lasers Opt.* **70**, 587–591 (2000)
4. P.K. Shen, J. Syed-Bokhari, A.C.C. Tseung, The performance of electrochromic tungsten trioxide films doped with cobalt or nickel. *J. Electrochem. Soc.* **138**, 2778–2783 (1991)
5. S.V. Green, E. Pehlivan, C.G. Granqvist, G.A. Niklasson, Electrochromism in sputter deposited nickel-containing tungsten oxide films. *Sol. Energy Mater. Sol. Cells* **99**, 339–344 (2012)
6. S.H. Lee, S.K. Joo, Electrochromic behavior of Ni–W oxide electrodes. *Sol. Energy Mater. Sol. Cells* **39**, 155–166 (1995)
7. S.-H. Lee, H.M. Cheong, N.-G. Park, C.E. Tracy, A. Mascarenhas, D.K. Benson, S.K. Deb, Raman spectroscopic studies of Ni–W oxide thin films. *Solid State Ionics* **140**, 135–139 (2001)
8. B. Sasi, K.G. Gopchandran, P.K. Manoj, P. Koshy, P.P. Rao, V.K. Vaidyan, Preparation of transparent and semiconducting NiO films. *Vacuum* **68**, 149–154 (2002)
9. T. Seike, J. Nagai, Electrochromism of 3d transition metal oxides. *Sol. Energy Mater.* **22**, 107–117 (1991)
10. P.K. Pandey, N.S. Bhave, R.B. Kharat, Preparation and characterization of nanostructured NiO thin films by reactive-pulsed laser ablation technique. *Electrochim. Acta* **51**, 4659–4664 (2006)
11. B. Sasi, K.G. Gopchandran, Preparation and characterization of nanostructured NiO thin films by reactive-pulsed laser ablation technique. *Sol. Energy Mater. Sol. Cells* **91**, 1505–1509 (2007)
12. S.V. Green, A. Kuzmin, J. Purans, C.G. Granqvist, G.A. Niklasson, Structure and composition of sputter-deposited nickel-tungsten oxide films. *Thin Solid Films* **519**, 2062–2066 (2011)
13. H.L. Chen, Y.M. Lu, W.S. Hwang, Thickness dependence of electrical and optical properties of sputtered Nickel oxide films. *Thin Solid Films* **514**, 361–365 (2006)
14. A. Mendoza-Galvan, M.A. Vidales-Hurtado, A.M. Lopez-Beltran, Comparison of the optical and structural properties of nickel oxide-based thin films obtained by chemical bath and sputtering. *Thin Solid Films* **517**, 3115–3120 (2009)
15. M.C. Rao, O.M. Hussain, Optical properties of vacuum evaporated WO_3 thin films. *Res. J. Chem. Sci.* **1**, 76–80 (2011)
16. H.R. Fallah, M. Ghasemi, A. Hassanzadeh, Influence of heat treatment on structural, electrical, impedance and optical properties of nanocrystalline ITO films grown on glass at room temperature prepared by electron beam evaporation. *Physica E* **39**, 69–74 (2007)
17. J.I. Pankove, *Optical Process in Semiconductors* (Prentice Hall, Inc., New Jersey, 1971), pp. 34
18. E. Burstein, Anomalous optical absorption limit in InSb. *Phys. Rev.* **93**, 632–633 (1954)
19. T.S. Moss, The interpretation of the properties of Indium antimonide. *Proc. Phys. Soc. London, Sect. B* **67**, 775–782 (1954)
20. M.A. Hassan, C.A. Hogarth, A study of the structural, electrical and optical properties of copper tellurium oxide glasses. *J. Mater. Sci.* **23**, 2500–2504 (1988)
21. N.F. Mott, E.A. Davis, *Electronic Processes in Non-Crystalline Materials* (Clarendon Press, Oxford, 1979)
22. Dirk Poelman, Philippe Frederic Smet, methods for the determination of the optical constants of thin films from single transmission measurements: a critical review. *J. Phys. D Appl. Phys.* **36**, 1850–1857 (2003)
23. N.A. Subrahmanyam, *A Textbook of Optics*, 9th edn. (Brj Laboratory, India, 1977)
24. A.A. Al-Ghamdi, W.E. Mahmoud, S.J. Yagmour, F.M. AlMarzouki, Structure and optical properties of nanocrystalline NiO thin film synthesized by sol-gel spin-coating method. *J. Alloys Compd.* **486**, 9–13 (2009)
25. J. Singh, *Optical Properties of Condensed Matter and Applications* (John Wiley & Sons, Chichester, 2006)
26. P.J.L. Herve, L.K.J. Vandamme, Empirical temperature dependence of the refractive index of semiconductors. *J. Appl. Phys.* **77**, 5476–5477 (1995)
27. W.L. Bragg, A.B. Pippard, The form birefringence of macromolecules. *Acta Crystallogr.* **6**, 865–867 (1953)
28. H.A. Macleod, Structure related optical properties of thin films. *J. Vac. Sci. Technol., A* **4**, 418–422 (1986)
29. *Optical Properties of Solids*, edited by F. Abeles (North-Holland Publishing Company, Amsterdam, London, 1972)
30. J.I. Pankove, *Optical Processes in Semiconductors* (Dover Publications Inc., New York, 1975), p. 91
31. T.S. Moss, G.J. Burrell, E. Ellis, *Semiconductor Opto-Electronics* (Butterworth's Scientific Publication LTD, London, 1973)
32. M. Abdel-Baki, F.A. Abdel, F. Wahab, El-Diasty, optical characterization of $x\text{TiO}_2-(60-x)\text{SiO}_2-40\text{Na}_2\text{O}$ glasses: I. Linear and nonlinear dispersion properties. *Mater. Chem. Phys.* **96**, 201–210 (2006)
33. M. Caglar, S. Ilican, Y. Calgan, Y. Sahin, F. Yakuphanoglu, D. Hur, A spectro electrochemical study on single-oscillator model and optical constants of sulfonated polyaniline film. *Spectrochimica Acta A* **71**, 621–627 (2008)
34. S.H. Wemple, M. DiDomenico, Behavior of the electronic dielectric constant in covalent and ionic materials. *Phys. Rev. B* **3**, 1338–1342 (1971)
35. D.K. Madhup, D.P. Subedi, A. Huczko, Influence of doping on optical properties of ZnO Nanofilms, *Optoelectron. Adv. Mater. Rapid Commun.* **4**, 1582–1586 (2010)
36. S.H. Wemple, Material dispersion in optical fibers. *Appl. Opt.* **18**, 31–35 (1979)
37. T. Wagner, M. Krbal, T. Kohoutek, V. Peina, M. Vlek, M. Frumar, Kinetics of optically- and thermally-induced diffusion and dissolution of silver in spin-coated $\text{As}_{33}\text{S}_{67}$ amorphous films; their properties and structure. *J. Non-Cryst. Solids* **326**, 233–237 (2003)
38. A. Kuzmin, J. Purans, R. Kalendarev, Local structure and vibrational dynamics in NiWO_4 . *Ferroelectrics* **258**, 21–30 (2001)

39. R. Sivakumar, C. Sanjeeviraja, M. Jayachandran, R. Gopalakrishnan, S.N. Sarangi, D. Paramanik, T. Som, Modification of WO_3 thin films by MeV N^+ -ion beam irradiation. *J. Phys.: Condens. Matter* **19**, 186204–186213 (2007)
40. C. Diaz-Guerra, A. Remon, J. Garcia, J. Piqueras, Cathodoluminescence and photoluminescence spectroscopy of NiO. *Phys. Stat. Sol. (a)* **163**, 497–503 (1997)
41. Yude Wang, Chunlai Ma, Xiaodan Sun, Hengde Li, Preparation and photoluminescence properties of organic–inorganic nanocomposite with a mesolamellar nickel oxide. *Microporous Mesoporous Mater.* **71**, 99–102 (2004)
42. D. Adler, J. Feinleib, Electrical and optical properties of narrow-band materials. *Phys. Rev. B* **2**, 3112–3134 (1970)
43. S.M.M. Zawawi, R. Yahya, A. Hassan, H.N.M. Ekramul Mahmud, M.N. Daud, Structural and optical characterization of metal tungstates (MWO_4 ; M = Ni, Ba, Bi) synthesized by a sucrose-templated method. *Chem. Cent. J.* **7**, 80–90 (2013)
44. E.G. Lee, M.D. Kim, D. Lee, Effect of the carrier capture process on the photoluminescence intensity and the decay time of semiconductor quantum dots. *J. Korean Phys. Soc.* **48**, 1228–1232 (2006)
45. T.S. Shyju, S. Anandhi, R. Sivakumar, S.K. Garg, R. Gopalakrishnan, Investigation on structural, optical, morphological and electrical properties of thermally deposited lead selenide (PbSe) nanocrystalline thin films. *J. Cryst. Growth* **353**, 47 (2012)